Modeling Hormonal Control of Cambium Proliferation

Vladyslav Oles[1], Alexander Panchenko[1,*], Andrei Smertenko[2,*],

1 Department of Mathematics, Washington State University, Pullman, Washington, USA
2 Institute of Biological Chemistry, Washington State University, Pullman, Washington, USA

***andrei.smertenko@wsu.edu; panchenko@math.wsu.edu**

Abstract

Rise of atmospheric CO_2 is one of the main causes of global warming. Catastrophic climate change can be avoided by reducing emissions and increasing sequestration of CO_2. Trees are known to sequester CO_2 during photosynthesis, and then store it as wood biomass. Thus, breeding of trees with higher wood yield would mitigate global warming as well as augment production of renewable construction materials, energy, and industrial feedstock. Wood is made of cellulose-rich xylem cells produced through proliferation of a specialized stem cell niche called cambium. Importance of cambium in xylem cells production makes it an ideal target for the tree breeding programs; however our knowledge about control of cambium proliferation remains limited. The morphology and regulation of cambium differs from stem cell niches that control axial growth. For this reason, translating the knowledge about axial growth to radial growth has limited use. Furthermore, genetic approaches cannot be easily applied because overlaying tissues conceal cambium from direct observation and complicate identification of mutants. To overcome the paucity of experimental tools in cambium biology, we constructed a Boolean network CARENET (CAmbium Regulation gene NETwork) for modelling cambium activity, which includes the key transcription factors WOX4 and HD-ZIP III as well as their potential regulators. Our simulations revealed that: (1) auxin, cytokinin, gibberellin, and brassinosteroids act cooperatively in promoting transcription of *WOX4* and *HD-ZIP III*; (2) auxin and cytokinin pathways negatively regulate each other; (3) hormonal pathways act redundantly in sustaining cambium activity; (4) individual cells in the stem cell niches can have diverse molecular identities. CARENET can be extended to include components of other signalling pathways and be integrated with models of xylem and phloem differentiation. Such extended models would facilitate breeding trees with higher wood yield.

Introduction

Competition for solar energy drives axial growth in many plant species resulting in stem elongation. However, longer stems become vulnerable to the forces of gravity and wind. Furthermore, efficiency of photosynthesis in leaves depends on the long-range transport of water and minerals from roots to shoots through the stem. Photoassimilates produced in leaves have to be transported back to roots. Hence, longer stems impose constraints on photosynthesis and growth. In the course of evolution, plants developed mechanisms that balance axial growth with radial (secondary) growth. One of the main

outcomes of radial growth is formation of xylem and phloem. Hollow xylem cells reinforced with thick secondary cell walls provide mechanical strength to the stem and a means of root-to-shoot transport. Phloem is responsible for shoot-to-root transport. A specialized meristem located between xylem and phloem, the cambium, divides periclinally to produce precursors for the xylem and phloem cells [1]. Despite significant progress in understanding molecular mechanisms of xylem differentiation and secondary cell wall synthesis, our knowledge about regulation of cambium activity remains scant.

The location of cambium between xylem and phloem facilitates integration of hormonal signals that are produced by both roots and shoots and their translation into secondary growth [2]. Consequently, activity of cambium is known to be regulated non-cell-autonomously by a complex signaling network [3] under control of auxin [4], cytokinin [5], ethylene [6], gibberellins [7], brassinosteroids [8], strigolactones [9] as well as signaling peptides CLE41, CLE42, CLE44 collectively called Tracheary Elements Differentiation Inhibition Factor (TDIF) [10, 11]. However, it remains unclear how complex hormonal signals are integrated by the genetic network that controls cambium.

The best studied signaling module controlling cambium proliferation consistes of TDIF receptor, Phloem Intercalated with Xylem (PXY), a Leucine Rich Repeat domain Receptor-Like Kinase (LRR-RLK) [10, 12], and transcription factors WOX4, WOX14 [13–15] and HD-ZIPIII (represented by ATHB-8 in *Arabidopsis*) [16–18]. While *PXY, WOX4,* and *WOX14* are cambium-specific genes, *HD-ZIPIII* is expressed in both cambium and immature xylem cells. TDIF is synthesized in phloem and then diffuses through the apoplastic space to cambium cells where it binds to the receptor domain of PXY [10, 19]. Activated PXY promotes expression of *WOX4, WOX14* [13–15], and *ATHB-8* [20]. PXY also phosphorylates and activates GSK3 kinase BIN2 [21]. Phloem is recalcitrant to TDIF signal because transcription of *PXY* in this tissue is inhibited by KANADI [22].

Although numerous lines of evidence support the essential role of PXY/WOX4 signaling module in the regulation of cambium proliferation [23], many questions remain unanswered. First, how is the TDIF signal integrated with other signals? For example, it has been shown that PXY/WOX4 module is also controlled by ethylene [24] and auxin [15]. Second, how are auxin and ethylene signaling integrated with gibberellic acid and brassinosteroids pathways which also control activity of cambium [7, 8]? Third, what makes cambium dormant during the cold season or inactive towards the end of developmental cycle in annual and perennial species?

Understanding the biology of cambium remains incomplete because cambium is concealed under phloem, epidermis, and cortex tissues. This hinders identification of mutants with altered secondary growth and identification of genes that control cambium activity. Furthermore, isolation of live cambium cells has not been achieved thus far. Mathematical modelling can help in predicting the outcome of interactions between components of complex genetic networks. For example, models have been developed for understanding identity of tissues in *Arabidopsis* vascular bundles [20] or for differentiation of xylem cells [25, 26]. However, a model of cambium proliferation has not been created thus far.

Here we describe a network model composed of known regulators of procambium or cambium development and activity, which we call CARENET (CAmbium REgulation gene NETwork). CARENET is a Boolean network of the type originally introduced by Kauffman [27–30]. Such models can be constructed on the basis of mostly qualitative information concerning the cause-and-effect relationships between pairs of agents (e.g. gene A activates or inhibits gene B). Since this type of information is commonly available in the biological literature, Boolean models have an advantage over other types of models (e.g. Ordinary Differential Equations; ODEs) construction of which may require relatively hard to obtain information about reaction rates. Additional

information on the analysis and simulation of Boolean networks in biology can be found in the books by Shmulevich and Dougherty [31, 32] and in the papers [33, 34].

In this work CARENET is primarily used for unraveling interactions between different hormonal signaling pathways for the control of secondary growth. Our simulation experiments accurately represent experimental data on the importance of cytokinin, auxin, and ethylene for cambium activity and demonstrate the ability of gibberellic acid and brassinosteroids to increase activity of cambium. Our model can be used for designing plants with altered secondary growth and biomass yield.

Materials and Methods

Software implementation

All simulations of cambium cell were performed using software designed specifically for this study. The program was implemented using Python 2.7 language. It embeds theoretically developed update rules for the model (S1 Table). Primary functionality of the program is to simulate the evolution of production of relevant chemicals in a cambium cell.

The software incorporates a feature that allows application of so-called "control actions", which manually override the state of any chosen node at any time step. This feature allows simulation of the effect of gene knockout. For instance, control actions forcing PXY node into the state of 0 at every time step of simulation simulates *pxy* mutant.

The program can process multiple initial states of the model in bulk, automatically calculating statistical data for each of the final states found. A single run tests all possible initial states for a specific configuration. Although such automation speeds up the process, simulations are computationally intensive due to the model size: processing of one control configuration required about two hours on a desktop computer.

Chi-squared test of independence

In order to test statistical significance of the relationships between intracellular hormone accumulation (activity) and proliferation activity (defined in Section "Numerical experiments and their statistical analysis"), or accumulation of another hormone, we use a test of independence, which is a version of the Pearson's chi-squared test. Since activity is a continuous variable taking values between 0 and 1, and the test only applies to categorical data, we bin this range into several equal parts, e.g., $[0, 0.25]$, $[0.25, 0.5]$, $[0.5, 0.75]$, $[0.75, 1]$. For the control nodes categorization is straightforward, as they can only take values 0 or 1.

Once the values of both variables under consideration are categorized, a contingency table matching categories of one variable with categories of another is constructed. Each cell of the table corresponds to a pair of categories and stores the number of instances for which the variables belong to the respective categories. The null hypothesis states the variables are independent, hence the expected numbers are equal in each cell. Afterwards, the sum of normalized squared deviations of observed numbers from the expected numbers is calculated to obtain the chi-squared test statistic (χ^2). Its critical value is determined by the degrees of freedom and chosen significance level, which represents the cut-off value for the likelihood of obtaining the experimental result by chance. We set the significance level to 0.05 (5%), commonly accepted as the optimal value. Comparing χ^2 to the critical value tells us whether we should accept or reject the null hypothesis.

A conclusion to reject the null hypothesis means that two variables are related. In such a case, we estimate whether their correlation is positive or negative. The distributions of activity levels of one variable are compared amongst themselves as another variable changes its activity level from lower to higher. If the first variable gets fewer cases of low activity and more cases of high activity as the second variable increases its level, the correlation is considered to be positive. Conversely, the correlation is considered negative if the above occurs for lower activity of the second variable.

Results

Constructing a model for the cambium-regulating gene network

To model cambium activity in response to developmental cues we choose a Boolean approach because it has been shown to produce reliable models of complex interactions even in the absence of quantitative data on concentration of relevant chemicals [34–36]. Here, cambium proliferation is modeled by a deterministic Boolean network (or graph) consisting of nodes and edges (Fig 1). Selection of the nodes and edges is based on information collected from published data on diverse developmental processes including leaf venation, primary growth of roots and stems, and secondary growth of stems and cotyledons in *Arabidopsis*, poplar, and peas (S2 Table). While nodes represent hormones, proteins, genes or cellular processes, the edges represent functional interactions between the nodes. An edge directed from node A to node B represents a cause and effect relationship between these nodes whereby node A either activates node B or inhibits it. Thus, each edge in our model is designated as inhibitory or activatory.

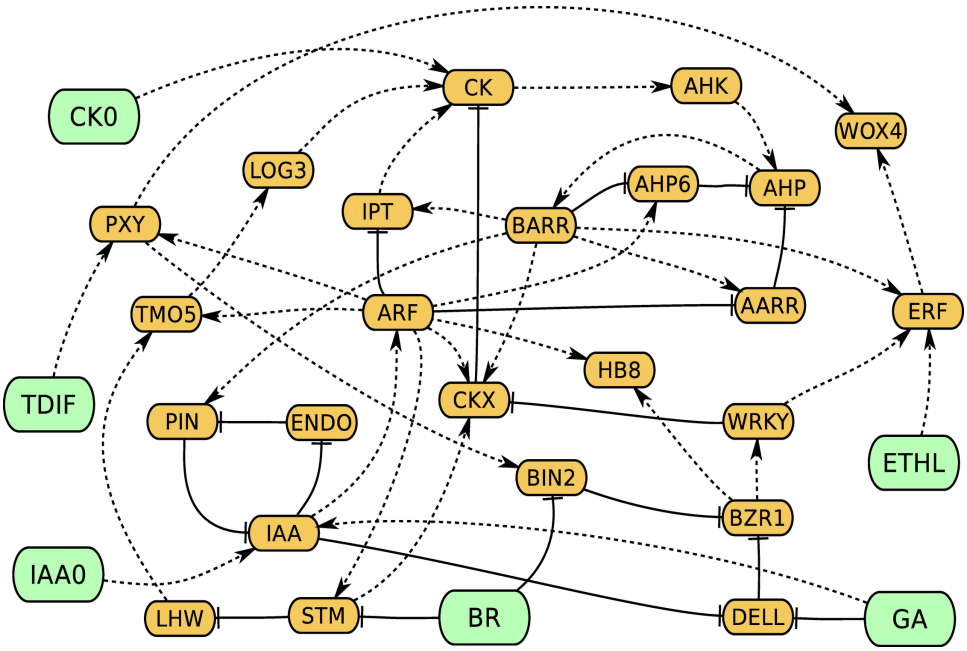

Fig 1. Cambium regulation gene network (CARENET). Control nodes are in green and internal nodes are in orange. Dashed and solid lines indicate activation and inhibition respectively. ATHB8 is labelled as HB8, ENDO means endocytosis.

Inclusion of nodes and edges inferred from research on divergent systems is justified by recent studies which demonstrate similarity of molecular mechanisms underlying cambium activity. For example, PXY-dependent signaling promotes cambium in *Arabidopsis* and poplar [14, 19, 37]. Below we describe the main signaling blocks of the CARENET and justification for inclusion of specific nodes and edges.

Cytokinin (CK). Mutations in genes encoding cytokinin synthesis enzymes (e.g. isopentenyltransferase; IPT) or receptors of cytokinin (Arabidopsis Histidine Kinase; AHK) exhibit reduced xylem content [5, 38–40]. Cytokinin can be synthesized locally and work in a cell-autonomous manner [41] or be transported for long distances through symplastic connections in phloem and act in a non-cell-autonomous fashion [42]. We introduced external (CK0) and internal (CK) nodes to represent both sources of cytokinin. Intracellular homeostasis of cytokinin is maintained through the balance of biosynthesis by IPT and cytokinin nucleoside 5-monophosphate phosphoribohydrolase (LOG), and deactivation by cytokinin oxidase (CKX). The downstream signaling processes contain a self-inhibitory mechanism: CKX transcription is up-regulated through B-type response regulator (RRB) ARR2 [43]. In addition to these components our network also includes AHP, type-A response regulator (RRA), and inhibitor of cytokinin signaling AHP6 (S2 Table). The heterodimer of transcription factors TMP5-LHW contributes to the cytokinin signaling network by promoting cytokinin synthesis through transcriptional activation of LOG3/4 [44].

Auxin (IAA). Auxin transported from shoots and secreted by the surrounding cells (IAA0) is taken up by cambium cells (IAA). The concentration of auxin was found to be the highest in cambium zone of poplar stems [4]. Decapitation of *Arabidopsis* plants shuts down the auxin supply from the shoots and reduces cambium activity while application of exogenous auxin reconstitutes cambium activity [45]. Furthermore, mutants with reduced sensitivity to auxin (e.g. *auxin resistant 1*), exhibit lower activity of interfascicular cambium [9]. Perception of the auxin signal ultimately results in activation of transcriptional regulators Auxin Response Factors (ARF; reviewed in [46]). As the bulk of auxin is produced in the shoots, transport becomes an essential part of the signaling network. Consequently, plants have evolved several auxin transporters amongst which are efflux carriers PIN proteins [47]. Four members of the PIN gene family *PIN1,5,6,* and *8* express in vasculature and play an important role in vasculature patterning [48, 49]. PINs in the surrounding tissues would promote cambium activity by increasing auxin concentration in cambium cells. However, up-regulation of PIN proteins in cambium cells would promote auxin efflux, thus causing reduction of intracellular auxin concentration (IAA) and inhibition of cambium proliferation. In our model, PINs are included in the negative feedback mechanism of intracellular auxin concentration (IAA).

Auxin and cytokinin cross-talk. Auxin and cytokinin reciprocally control their intracellular concentration (IAA and CK) through negative feedback loops. Antagonistic relationships between these hormones defines cambium division rate and the vascular tissue pattern in roots [50, 51]. Auxin can cause a reduction of intracellular cytokinin by promoting expression of a key deactivating enzyme CKX [52] and by down-regulating transcription of an essential biosynthetic enzyme *IPT* [53, 54]. In agreement with these observations, treatment with auxin reduces several major cytokinin intermediates [53]. Furthermore, ARFs promote transcription of *AHP6* which inhibits cytokinin signaling [50, 55].

Cytokinin can potentially diminish availability of auxin to cambium cells through RRB-dependent down-regulation of PIN expression in the surrounding tissues [42, 56].

Moreover, cytokinin can reduce the concentration of auxin in cambium cells by up-regulating expression of PIN proteins [57, 58], which depends on binding of the Cytokinin Response Factors (CRFs) to a specific region of *PIN* promoter [59]. In our model cytokinin dampens auxin signaling through RRB-dependent up-regulation of PINs expression and subsequent increase in auxin efflux. This negative feedback loop maintains hormonal balance in cambium under steady state conditions.

Relationships between auxin and cytokinin can be cooperative. In our model ARF promotes transcription of *TMO5* which together with LHW up-regulates expression of a key cytokinin biosynthesis enzyme *LOG3/4* [51]. At the same time, ARF can inhibit transcription of *LHW* through transcriptional activation of *STM* (Fig 1; [60, 61]). It has also been shown that STM may play a role in xylem cells differentiation [62].

Ethylene (ETHL). Ethylene was implicated in secondary growth because transcription of genes encoding Ethylene-Responsive transcription Factors (ERF) are up-regulated in cambium proliferation mutants *pxy* and *wox4* [24]. In agreement with this suggestion, *ERFs* knockout exacerbates the reduced xylem phenotype in *pxy* and reduces transcription level of *WOX4*. These findings indicate that ethylene signaling cooperates with PXY to control WOX4-dependent proliferation of cambium.

Brassinosteroids (BR). Overexpression of the brassinosteroids receptor BRI1 promotes proliferation of cambium and increases the amount of xylem in vascular bundles [63]. A similar phenotype was observed in plants expressing constitutively active BRI1 [8, 64]. BRI1 was omitted in the model because brassinosteroids signal ultimately inhibits protein kinase activity of BIN2. Consequently, degradation of transcription factors *BRASSINAZOLE RESISTANT 1 (BZR1)* and *bri1-EMS-SUPPRESSOR 1 (BES1)* is inhibited and they promote transcription of the targets [65]. Only BZR1 was retained in the network because these transcription factors were considered functionally redundant in regulating cambium proliferation. The connection between brassinosteroids pathway and PXY/WOX4 module remains unknown and we propose transcription factors of WRKY family as a potential bridge. This hypothesis is justified by three independent observations. First, *WRKY12* is down-regulated in the *bri1* background [66]. Second, according to the publicly available microarray data, transcription of *WRKY12* is up-regulated by BR. Third, ectopic expression of constitutively active mutant BRI1Y831F up-regulates transcription of *WRKY48* [8]. We also propose a connection between WRKY and PXY/WOX4 module through ERF considering the observation that knockout of *Medicago truncatula WRKY12* homologue leads to down-regulation of *ERF4* [67].

Gibberellic acid (GA) and crosstalk between GA, BR, and IAA pathways. Over-production of GA in transgenic poplar expressing GA 20-oxidase, an enzyme responsible for GA-biosynthesis, promotes cambium proliferation [7]. Application of GA to decapitated poplar trees also stimulates proliferation of cambium [68]. The GA-signaling pathway was suggested to promote secondary growth during flowering in *Arabidopsis* because xylem content was three times lower in GA biosynthesis mutant *ga1-3* [69]. The underlying mechanism of interaction between GA signaling and the PXY/WOX4 module remains unknown. Experimental data suggests that cross-talk of the TDIF/PXY signaling module with brassinosteroids and gibberellic acid could be facilitated by members of the WRKY family of transcription factors. In addition to the arguments given in "Brassinosteroids (BR)" paragraph, transcription of *WRKY12, WRKY48*, and *WRKY53* is up-regulated by brassinosteroids according to publicly available microarray data. Furthermore, *WRKY12* is up-regulated by gibberellic acid. WRKY also links brassinosteroids and gibberellic acid with cytokinin signaling by

inhibiting transcription of the cytokinin-degrading enzyme *CKX* [67] and by promoting the LHW-dependent transcription of a gene that encodes the cytokinin biosynthetic enzyme *LOG3/4* [61,66]. Björklund et al. have shown that GA can activate IAA signaling in cambium by promoting expression of PIN1 in the cells at the early xylem differentiation stages [68]. This would ultimately result in higher IAA concentration in cambium cells.

Model implementation

The nodes of the network are denoted by $V_1, V_2, \ldots, V_N$, where $N = 30$ is the number of nodes. The changes in gene expression level or concentration of a chemical are modeled by assigning a state s_i to the corresponding node V_i, $i = 1, \ldots, N$. At each instant of time, a state s_i equals either 0 or 1. The value 0 indicates low activity level, while the value 1 indicates high activity level.

The nodes are divided into two groups: control nodes and internal nodes (Fig 1). Control nodes represent hormonal/peptidic signals produced by surrounding or remote tissues (CK0, IAA0, BR, GA, TDIF, and ETHL). These nodes are not influenced by other nodes in the network. Internal nodes can be regulated by both the control nodes and other nodes in the network. The states of control nodes remained fixed throughout each simulation run, while the states of internal nodes may vary.

As mentioned in Section "Constructing a model for the cambium-regulating gene network", functional interactions between the nodes are represented by edges. An edge directed from V_i to V_j encodes the following assumptions: (i) there is a chain of chemical reactions where V_i is an input and V_j is a product; (ii) the reactions producing V_j from V_i may involve other chemicals but these chemicals are not included into the model; and (iii) these intermediate chemicals do not influence the states of other nodes. An activatory edge from V_i to V_j is denoted by $(V_i \longrightarrow V_j)$ and an inhibitory edge is denoted by $(V_i \dashv V_j)$.

Update rules

The state of each node changes in time according to the update rules. The next value s_i is determined by the current value s_j of every node affecting V_i by means of an edge directed from V_j to V_i. In order to describe the rules in detail, we use the following notations. Each edge from V_j to V_i is assigned a weight

$$w_{ij} = \begin{cases} 1 & \text{if } V_j \text{ activates } V_i, \\ -1 & \text{if } V_j \text{ inhibits } V_i. \end{cases}$$

Furthermore we define an auxiliary function $r_i = \sum_{j \in \mathcal{I}_i} s_j w_{ij}$, where $\mathcal{I}_i$ is the set of indices of all nodes influencing V_i. Detailed explanation of the role of r_i in calculating the rules will be provided below. Suppose that there are n_i nodes affecting V_i, of which m_i nodes are inhibitory. As the states s_j of these nodes are either 0 or 1, the range of r_i is the interval $[-m_i, n_i - m_i]$. The smallest value $-m_i$ is obtained when the state of every inhibitory node is 1, and the state of every activatory node is 0. The largest value $n_i - m_i$ corresponds to the reverse situation.

To calculate the value of s_i at the next step we compute r_i using current values of s_j and then apply the following rule:

$$s_i = \begin{cases} 1 & \text{if } r_i > \frac{n_i}{2} - m_i, \\ 0 & \text{otherwise.} \end{cases} \quad (1)$$

Equation (1) means that s_i will take the value 1 if r_i is greater than the arithmetic mean of end point values of the interval $[-m_i, n_i - m_i]$, otherwise s_i will take the value 0.

To illustrate the process of updating the node states using the above rules, we provide an example in which a node V_i is influenced by nodes V_1, V_2 and V_3. Suppose that V_1 and V_2 activate V_i, while V_3 inhibits it (Fig 2A). Therefore, there are three edge weights $w_{i1} = 1$, $w_{i2} = 1$, and $w_{i3} = -1$, and thus $n_i = 3$ and $m_i = 1$. The next value of s_i calculated from the current values of s_1, s_2 and s_3 according to (1) is shown in Fig 2B.

A

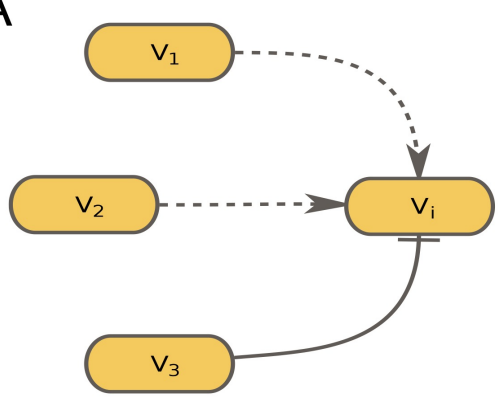

B

s_1	s_2	s_3	r_i	s_i
0	0	0	0	0
0	0	1	−1	0
0	1	0	1	1
0	1	1	0	0
1	0	0	1	1
1	0	1	0	0
1	1	0	2	1
1	1	1	1	1

Fig 2. Interaction rules between the nodes.
A, Example of a node V_i influencing nodes V_1, V_2 and V_3.
B, Values of r_i and s_i for all possible combinations of s_1, s_2 and s_3.

Remark on why the inequality in (1) *is strict.*

When $r_i = \frac{n_i}{2} - m_i$, the value of s_i obtained from the formula (1) equals 0. This choice is motivated by the special case in which a node V_i is influenced by two nodes connected by activatory edges. When one of them is active and the other is inactive, the resulting $r_i = \frac{2}{2} - 0 = 1$, which is the midpoint of the range interval $[0, 2]$. Assuming that both nodes must be active in order for $s_i = 1$, in this case the node V_i should be inactive ($s_i = 0$). For the sake of consistency, we adopt the same rule for the general case of n_i nodes: if $r_i = \frac{n_i}{2} - m_i$, then $s_i = 0$.

Numerical experiments and their statistical analysis

Simulating dynamics of genetic networks requires information on the initial conditions. However, limited time resolution of currently available assays of gene transcription and protein turnover rate in cambium precludes generating sufficiently accurate datasets that could be used as initial conditions. Hence, information about behavior of the network is generated by repeatedly simulating its dynamics under all possible initial conditions. A single simulation run consists of the following steps. First, each control node is assigned a specific state. Combination of such assignments for all control nodes constitutes a *control state*. Once chosen, the control state remains fixed throughout the course of the run. Second, initial states are assigned to the internal nodes. Third, the states of all internal nodes are updated according to the rules described above.

The states of the internal nodes are updated sequentially until a *final state* is attained. In this state the network either remains completely static (a steady state), or cycles through a finite number of states (a limit cycle). As the outcome of a run we record the initial conditions (initially assigned states of the internal nodes), the control

state, and the final state. Then, the initial conditions and the controls are modified and a new run commences. The simulation stops once all combinations of the initial conditions and all control states have been exhausted. The final states provide reliable information about behavior of the network, while transient states are considered uninformative because Boolean dynamical systems lack physically relevant time scales [20, 70].

Each numerical experiment consists of many runs performed with the same values of controls and different initial conditions for the internal nodes. Although the final states obtained for specific initial conditions could potentially be different, many initial conditions lead to the same final state. Hence, the number of final states compatible with a given control state is smaller (typically orders of magnitude smaller) than the number of all possible initial conditions. This suggests that the number of initial conditions leading to a particular final state can be used to characterize its persistence relative to other final states.

The lack of experimental data on the initial conditions of genetic networks is reminiscent of molecular dynamics where the initial positions and velocities of individual molecules can not be measured. Thus, observable quantities in molecular dynamics are produced by means of probabilistic (ensemble) averaging. Every set of initial positions and velocities is assigned a number reflecting the probability of occurrence. Then observed or simulated results corresponding to different initial conditions are averaged using these probabilities as weights.

Here, we develop a similar approach for interpreting dynamic behavior of Boolean networks. Within this approach, each final state F is assigned a weight

$$p(F) = \frac{I(F)}{2^{N_{\rm int}}} \tag{2}$$

where $I(F)$ is the number of initial conditions which lead to F and $N_{\rm int}$ is the number of interior nodes. The weight $p(F)$ takes values between 0 and 1 and the sum of $p(F)$ over all possible F equals 1. Thus $p(F)$ can be viewed as the probability of occurrence of the final state F. It is also worth noting that the assignment (2) is based on the assumption that all initial conditions are equiprobable. Such assignment of probabilities based on the size of attraction basins have been previously employed in [71] for studying the basin entropy of Boolean networks.

The relative importance of the node V_i in a final state F is described by the *activity* $\alpha_i(F)$, taking values between 0 and 1. If F is a steady state, $\alpha_i(F) = s_i$, so activity is either 0 or 1. If F is a limit cycle, a node state s_i may take the value 1 at some steps within the cycle, and take the value 0 at other steps. In this case, $\alpha_i(F)$ is determined by dividing the number of steps where $s_i = 1$ by the total length of the cycle. For example, if a limit cycle F consists of 7 update steps with 3 of them resulting in $s_i = 1$, then $\alpha_i(F) = \frac{3}{7}$.

Next, we define the average activity $\overline{\alpha}_i(C)$ associated with a control state C. It is calculated as a weighted mean of activities $\alpha_i(F_k)$ taken over all final states F_k related to C. Related final states are defined as states that are produced by simulating network dynamics with a fixed control state C and all possible initial conditions. Specifically,

$$\overline{\alpha}_i(C) = \sum_{k=1}^{K(C)} p(F_k)\alpha_i(F_k), \tag{3}$$

where $F_k,\ k = 1, \ldots, K(C)$ denote all final states related to C. By combining formulas (2) and (3) it can be easily seen that $\overline{\alpha}_i(C)$ is the arithmetic mean of the activities α_i resulting from each of $2^{N_{\rm int}}$ initial conditions (with the control state C being fixed).

Reporters of the CARENET activity. Available experimental data demonstrates that transcription levels of *WOX4* and *AtHB8* correlate with cambium proliferation and therefore can be used to assess the activity of CARENET. The transcription pattern of *WOX4* is spatially limited to (pro)cambium [14, 15, 72]. Furthermore, reduced cambium proliferation in *pxy* and ethylene signaling mutants *erf108erf109* is accompanied by lower *WOX4* transcription level [13, 24]. Another important argument for using *WOX4* as a reporter of cambium activity is that exogenous application of auxin in *wox4* background promoted transcription of *CLE44* (TDIF) peptide; however proliferation of cambium was not induced [15]. *AtHB8* is transcriptionally active in the pre-procambial cells of leaf veins [73] and *AtHB8* transcription also increases around damaged parts of stem [16]. Presence of *AtHB8* in the protoxylem and metaxylem domain of vascular bundles [50] suggests an additional role of AtHB8 in the transition of cambium cells from proliferation to differentiation.

Thus, two parameters can be potentially used to describe quantitatively the propensity of a control state C to induce proliferation: one relies on $\overline{\alpha}_{\mathrm{WOX4}}(C)$ only, and another that takes into account the activities of both nodes WOX4 $\overline{\alpha}_{\mathrm{WOX4}}(C)$ and AtHB8 $\overline{\alpha}_{\mathrm{ATHB\text{-}8}}(C)$. In the latter case, the average combined proliferation activity $\overline{\alpha}_{\mathrm{c}}(C)$ associated with C is defined as follows:

$$\overline{\alpha}_{\mathrm{c}}(C) = \sqrt{\frac{\overline{\alpha}^2_{\mathrm{WOX4}}(C) + \overline{\alpha}^2_{\mathrm{ATHB\text{-}8}}(C)}{2}}, \tag{4}$$

Overall Performance of the CARENET

Simulation of the CARENET using all possible combinations of control states and initial conditions (2^{30}) resulted in 204 final states. Amongst these, 152 states were limit cycles consisting of 2 to 18 steps (S3 Table). Several representative examples of the limit cycles and one steady state are shown in Fig 3 and S1-S3 Figs. Structure of the limit cycles shows periodic oscillations of cytokinin signaling nodes CK, AHK, or AHP irrespectively of the status of external cytokinin (CK0). These oscillations are enabled through the activity of nodes that produce (LOG3 and IPT) or degrade (CKX) cytokinin. Furthermore, statistical analysis of the final states revealed a negative correlation between IAA and CK (Table 1), which was independent of external auxin and cytokinin. These outcomes agree with the experimental data on the mutually inhibitory relationships between cytokinin and auxin signaling.

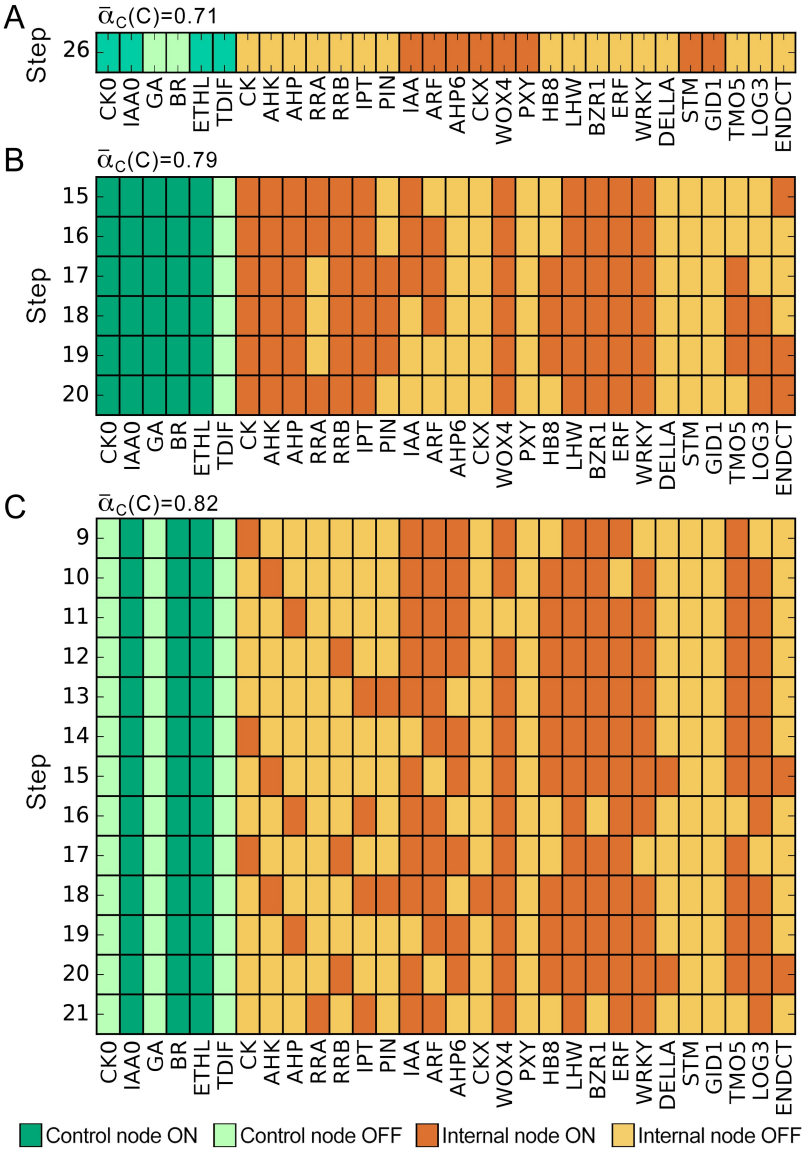

Fig 3. Representative examples of a stable state and limit cycles.

A, Stable state achieved by step 26.

B, C, Limit cycles established by step 15 or 9 respectively. Intracellular cytokinin (CK) synthesis oscillates even in the absence of external cytokinin CK0. ATHB8 is labelled as HB8.

As described earlier, two parameters can potentially be used for evaluating CARENET behavior: one that relies on the activity of WOX4 node, $\overline{\alpha}_{\mathrm{WOX4}}(C)$, and another one that takes into account activity of WOX4 and AtHB8 nodes, $\overline{\alpha}_{\mathrm{c}}(C)$. We found that $\overline{\alpha}_{\mathrm{WOX4}}(C)$ and $\overline{\alpha}_{\mathrm{c}}(C)$ are significantly correlated (Table 1). Therefore, $\overline{\alpha}_{\mathrm{WOX4}}(C)$ and $\overline{\alpha}_{\mathrm{c}}(C)$ can be used for assessing activity of CARENET interchangeably.

Table 1. Correlation analysis between control nodes and proliferation. Grey shading indicates statistically significant correlation between the variables (0.05 significance level).

Variable 1	Variable 2	Conditions	Relationships
IAA	CK	–	Negatively correlate with each other
IAA	CK	CK0 = 0, IAA0 = 1	Negatively correlate with each other
IAA	CK	CK0 = 1, IAA0 = 1	Negatively correlate with each other
$\overline{\alpha}_{\mathrm{c}}(C)$	$\overline{\alpha}_{\mathrm{WOX4}}(C)$	–	$\overline{\alpha}_{\mathrm{WOX4}}(C)$ positively correlates with $\overline{\alpha}_{\mathrm{c}}(C)$
CK	$\overline{\alpha}_{\mathrm{c}}(C)$	–	CK and are dependent, but the character of relationships could not be determined
IAA	$\overline{\alpha}_{\mathrm{c}}(C)$	–	IAA positively correlates with $\overline{\alpha}_{\mathrm{c}}(C)$
ETHL	$\overline{\alpha}_{\mathrm{c}}(C)$	–	ETHL positively correlates with $\overline{\alpha}_{\mathrm{c}}(C)$
GA	$\overline{\alpha}_{\mathrm{c}}(C)$	–	Test is inconclusive at 0.05 significance level
BR	$\overline{\alpha}_{\mathrm{c}}(C)$	–	BR positively correlates with $\overline{\alpha}_{\mathrm{c}}(C)$
TDIF	$\overline{\alpha}_{\mathrm{c}}(C)$	–	TDIF positively correlates with $\overline{\alpha}_{\mathrm{c}}(C)$
CK	$\overline{\alpha}_{\mathrm{c}}(C)$	TDIF = 1	CK positively correlates with $\overline{\alpha}_{\mathrm{c}}(C)$
IAA	$\overline{\alpha}_{\mathrm{c}}(C)$	TDIF = 1	IAA positively correlates with $\overline{\alpha}_{\mathrm{c}}(C)$
ETHL	$\overline{\alpha}_{\mathrm{c}}(C)$	TDIF = 1	ETHL positively correlates with $\overline{\alpha}_{\mathrm{c}}(C)$
GA	$\overline{\alpha}_{\mathrm{c}}(C)$	TDIF = 1	GA positively correlates with $\overline{\alpha}_{\mathrm{c}}(C)$
BR	$\overline{\alpha}_{\mathrm{c}}(C)$	TDIF = 1	BR positively correlates with $\overline{\alpha}_{\mathrm{c}}(C)$
CK	$\overline{\alpha}_{\mathrm{c}}(C)$	–	CK positively correlates with $\overline{\alpha}_{\mathrm{WOX4}}(C)$
IAA	$\overline{\alpha}_{\mathrm{WOX4}}(C)$	–	Test is inconclusive at 0.05 significance level
ETHL	$\overline{\alpha}_{\mathrm{WOX4}}(C)$	–	ETHL positively correlates with $\overline{\alpha}_{\mathrm{WOX4}}(C)$
GA	$\overline{\alpha}_{\mathrm{WOX4}}(C)$	–	Test is inconclusive at 0.05 significance level
BR	$\overline{\alpha}_{\mathrm{WOX4}}(C)$	–	Test is inconclusive at 0.05 significance level
TDIF	$\overline{\alpha}_{\mathrm{WOX4}}(C)$	–	TDIF positively correlates with $\overline{\alpha}_{\mathrm{WOX4}}(C)$
CK	$\overline{\alpha}_{\mathrm{WOX4}}(C)$	TDIF = 1	CK positively correlates with $\overline{\alpha}_{\mathrm{WOX4}}(C)$
IAA	$\overline{\alpha}_{\mathrm{WOX4}}(C)$	TDIF = 1	IAA positively correlates with $\overline{\alpha}_{\mathrm{WOX4}}(C)$
ETHL	$\overline{\alpha}_{\mathrm{WOX4}}(C)$	TDIF = 1	ETHL positively correlates with $\overline{\alpha}_{\mathrm{WOX4}}(C)$
GA	$\overline{\alpha}_{\mathrm{WOX4}}(C)$	TDIF = 1	GA positively correlates with $\overline{\alpha}_{\mathrm{WOX4}}(C)$
BR	$\overline{\alpha}_{\mathrm{WOX4}}(C)$	TDIF = 1	BR positively correlates with $\overline{\alpha}_{\mathrm{WOX4}}(C)$

Regulation of cambium activity by hormones

To examine the responsiveness of the CARENET to external signals, we measured the impact of individual hormones on cambium proliferation (S3 Table). In these experiments the control node in question was set at 1 while the rest of the control nodes varied. Then simulations were conducted using all possible initial conditions and the average proliferation activity was calculated. Constitutive activity of each hormone (=1) leads to higher $\overline{\alpha}_{\mathrm{WOX4}}(C)$ values relative to the situation when the hormone is inactive (equal 0; Fig 4A). Statistical analysis revealed that under conditions used, CK, ETHL, and TDIF positively correlated with $\overline{\alpha}_{\mathrm{WOX4}}(C)$; and CK, IAA, BR, ETHL, and TDIF positively correlated with $\overline{\alpha}_{\mathrm{c}}(C)$ at significance level 5% (Table 1). This outcome seems inconsistent with published experimental data on the importance of all hormones in cambium activity. However, as cambium tissue identity is maintained by TDIF/PXY signaling module, all hormonal signaling pathways most likely always incorporate this module. Therefore correlation between $\overline{\alpha}_{\mathrm{WOX4}}(C)$ and individual signals should be assessed while TDIF=1. Indeed, we found that all hormonal signals correlated with $\overline{\alpha}_{\mathrm{WOX4}}(C)$ or $\overline{\alpha}_{\mathrm{c}}(C)$ under these conditions. Moreover, TDIF could amplify the effect of each hormone on $\overline{\alpha}_{\mathrm{WOX4}}(C)$ (Fig 4B).

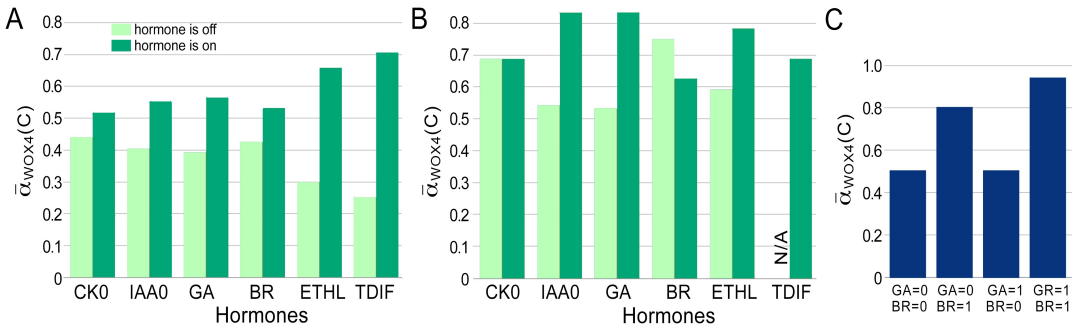

Fig 4. Effect of hormones on CARENET activity.

A, $\overline{\alpha}_{\mathrm{WOX4}}(C)$ obtained in the simulations experiments where corresponding hormone (control node) is turned on (dark green bars) or off (pale green bars).

B, $\overline{\alpha}_{\mathrm{WOX4}}(C)$ obtained in the simulations experiments where TDIF was always on (TDIF=1) and corresponding hormone is turned on (dark green bars) or off (pale green bars). N/A, not applicable.

C, Effect of gibberellins and brassinosteroids on $\overline{\alpha}_{\mathrm{WOX4}}(C)$ under conditions when the rest of the control nodes were on.

Next, we analyzed relationships between GA and and BR. It appears that GA could increase $\overline{\alpha}_{\mathrm{WOX4}}(C)$ to almost maximal value (1) in cooperation with BR, but not on its own (Fig 4C). These findings demonstrate synergistic relationships between gibberellic acid and brassinosteroids in promoting cambium proliferation.

To evaluate responsiveness of our system to changes in hormonal signals, we arbitrarily subdivided $\overline{\alpha}_{\mathrm{c}}(C)$ into four bins: no activity $0 < \overline{\alpha}_{\mathrm{c}}(C) < 0.25$; low activity $0.25 \leq \overline{\alpha}_{\mathrm{c}}(C) < 0.5$, medium activity $0.5 \leq \overline{\alpha}_{\mathrm{c}}(C) < 0.75$; and high activity $0.75 \leq \overline{\alpha}_{\mathrm{c}}(C) < 1$. With that calibration, medium activity was detected in 30 out of 64 possible control states, while high, low, and no activity was detected in 5, 4, and 25

control states respectively (S3 Table). $\overline{\alpha}_{\mathrm{WOX4}}(C)$ behaved similarly achieving high, medium, low, and no activity in 30, 4, 0, and 30 control states respectively (S3 Table). Underrepresentation of the control states resulting in the low activity suggests that response of CARENET to hormonal signals is based on all-or-none principle. Once proliferation is activated, the role of hormones would be modulating the relative activity according to the developmental or environmental situation.

The fact that different combinations of control nodes result in similarly high or medium $\overline{\alpha}_{\mathrm{c}}(C)$ values, emphasizes the redundancy of the hormonal signals in regulation of cambium activity. This situation is exemplified in Fig 3B,C where two different control states result in almost identical $\overline{\alpha}_{\mathrm{c}}$ values in structurally distinct final states. Furthermore, a given control state can also result in distinct final states with similar values of $\overline{\alpha}_{\mathrm{c}}$ for different initial conditions (S4 Fig). In the context of plant development these data suggest molecular heterogeneity of individual cells within the cambium.

Testing the effect of mutations

Sensitivity of CARENET to hormonal signals suggests that it can be used to predict the impact of mutations on cambium proliferation. To test this hypothesis, we simulated the effect of mutations known to reduce cambium proliferation: *pxy* knockout [10, 12]; double knockout of ERFs *erf108erf109* [24]; a quadruple knockout of IPT which was deficient in cytokinin synthesis [40]; and mutants in cytokinin receptor AHK4 [5, 38]. Mutations were mimicked by keeping the values of PXY, ERF, IPT or AHK at 0 throughout the simulations. The $\overline{\alpha}_{\mathrm{WOX4}}(C)$ failed to respond to TDIF in *pxy*, ethylene in *erf*, and to cytokinin in *ahp* and *ipt* (compare Fig 4A and Fig 5A-D). However, proliferation activity in these mutants responded to other signals. It demonstrates that corresponding nodes define sensitivity of the CARENET to specific external signals. In agreement with the experimental data, knockout of *PXY, ERF, AHK* and *IPT* resulted in lower proliferation activity (Fig 5F). These simulations demonstrate that CARENET represents experimental data on the functions of key signaling nodes in regulation of cambium proliferation. Next, we tested our hypothesis that BR controls activity of PXY/WOX4 module through WRKY by simulating *wrky* mutant. In agreement with our hypothesis *wrky* was insensitive to BR (Fig 5E) and exhibited lower proliferation activity than the control (Fig 5F).

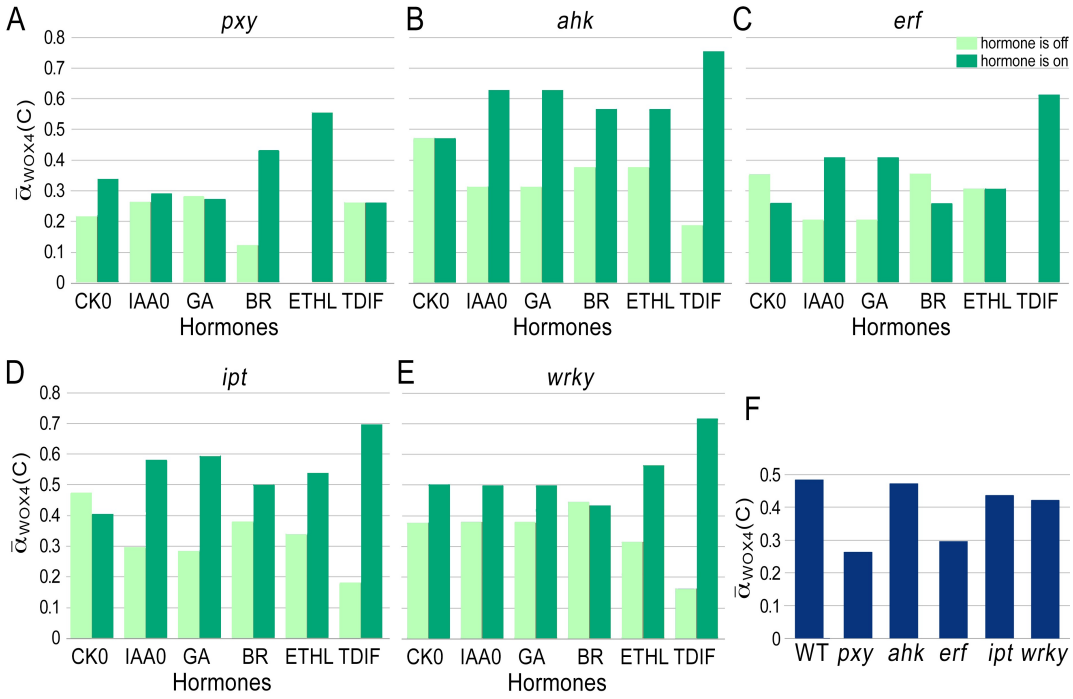

Fig 5. Effect of mutations on CARENET activity.

A-E, Simulating effect of hormones on $\overline{\alpha}_{\mathrm{WOX4}}(C)$ in *pxy, ahk, erf, ipt,* and *wrky* mutant backgrounds. $\overline{\alpha}_{\mathrm{WOX4}}(C)$ was averaged for all the simulations with the corresponding control node on (dark green bar) or off (pale green bar).

F, Proliferation in *pxy, ahk, erf, ipt,* and *wrky* mutant backgrounds.

Discussion

Hormonal cross talk in cambium regulation

The progress in understanding molecular mechanisms underlying cambium activity has benefited from analysis of procambium formation and vascular tissue patterning in *Arabidopsis* during embryogenesis, early post-embryonic growth [74, 75], and secondary growth [2, 23]. These efforts resulted in discovery of a number of genes responsible for each process. However, as mutations affecting procambium formation would also impact later cambium functions, the relevance of various sets of data for modeling cambium regulation requires further clarification [76]. In the absence of unequivocal experimental evidence to the contrary, it is reasonable to assume that these networks act in concert. Our computational experiments support the view that genetic mechanisms of procambium formation are likely to be exploited during secondary growth.

Our model combines the core cytokinin and auxin signaling modules employed by Benitez and Hejatko [20] with available experimental data on signaling mechanisms of ethylene, gibberellins, and brassinosteroids. One of the main challenges in this task was limited mechanistic data on the interaction between hormonal signals and the

PXY/WOX4 module. We addressed this challenge by incorporating several nodes and edges that link distinct signaling pathways.

The first important integrating component of the CARENET is represented by the key ethylene signaling component ERFs. Microarray and qRT-PCR analyses demonstrated significant up-regulation of *ERFs* in *pxy* mutant background [24]. Cambium proliferation phenotype in *pxy* and *wox4* alleles was mild suggesting that up-regulation of the ethylene pathway compensates for inactivity of the PXY/WOX4 module. However, reduction of *WOX4* transcription in *erf109erf018* double mutant was statistically insignificant [24] indicating that more than two members of *ERF* gene family are responsible for this regulation. We anticipate that analysis of high-order *ERF* mutants would demonstrate regulation of *WOX4* or its close homologue *WOX14* by ERFs.

In addition to controlling *WOX4* transcription, ERFs link PXY/WOX4 module with cytokinin signaling. Although the effect of cytokinin on *WOX4* transcription has not been examined, RRB2 can bind to the promoter of *ERF1* and stimulate its transcription [43]. Correspondingly, transcription of *ERF1* was down-regulated in *RRB* mutant allele *arr2* [43]. Higher transcription level of *ERF* in combination with ethylene would stimulate transcription of *WOX4* and result in higher cambium activity. Consistent with this prediction, *AHK4* knockout allele with reduced sensitivity to cytokinin exhibits lower cambium activity [5]. ERF could also serve as a link between PXY/WOX4 module and BR signaling. This hypothesis has been supported indirectly by the fact that *wrky12* knockdown results in transcriptional down-regulation of *ERF* [67]. More experimental data is needed to clarity the role of WRKY in the regulation of cambium activity.

Linking ETHL, BR, GA, and TDIF with the *bona fide* components of auxin and cytokinin signaling produced a network that accurately represents experimental data in showing additive effect of hormones on cambium activity and mimicking the effect of mutations in the key nodes. More nodes and edges can be added to the CARENET to facilitate understanding of how cambium proliferation changes in response to other hormones, mobile peptides, RNAs, environmental changes and nutrient availability.

Molecular heterogeneity of cambium cells

Being a typical Boolean network, CARENET lacks physical time scales. Therefore the number and structure of steps preceding establishment of the stable states or limit cycles shown in Fig 3, and S1-S4 Figs lack biological relevance. These steps depend on the structure of the network and the rules. Likewise, the number and structure of steps in the limit cycles are time-independent. However, activity of specific nodes in the limit cycles (i.e. the ratio of the number of steps at which a node acquires value 1 to the number of all steps in a cycle) is useful for converting the binary readouts of a Boolean network into a continuous scale. In turn, a continuous scale enables comparison of gene activity in distinct final conditions generated by different combinations of controls. Consequently, results of the simulations could be interpreted more accurately in a specific biological context.

Our simulations demonstrate that proliferation of cambium is controlled redundantly by hormonal signals (control nodes). For example the combination of CK0 and ETHL produced the same proliferation activity (0.7) as GA and TDIF (S3 Table). The effect of each signaling pathway appears to be additive and higher proliferation could be achieved when more pathways become active. This outcome supports available experimental evidence on the redundancy of mechanisms regulating developmental processes. Less expectedly, our simulations showed that identical control states may result in structurally distinct stable states with similar proliferation activity ($\overline{\alpha}_{\mathrm{c}}(C)$ or $\overline{\alpha}_{\mathrm{WOX4}}(C)$). Thus, individual cambium cells exhibiting the same proliferation activity

may possess distinct molecular identities. Such identities can be characterized by the different expression levels of the key regulatory genes. While activity of some pathways in the individual cells could be suboptimal, the proliferation would still be sustained by elevated activity of other pathways.

Temporal transcriptional analysis demonstrated that successive stages of lateral root meristem establishment are accompanied by sequential activation of different sets of genes [77]. Similar processes may take place during the establishment of all meristems. Nonetheless, subsequent activity of the stem cell niches including cambium and apical meristems can potentially undergo stochastic oscillations. Predicted molecular heterogeneity of cambium cells could also occur in other meristems and it would be interesting to verify this hypothesis using single-cell transcriptomics.

Limitations and future work

1. Currently the only receptor kinase in the CARENET is PXY. The role of PXY in the regulation of cambium proliferation was supported by the following observations: (i) reduction of cambium cell niche in *pxy/tdr1* mutants [10, 12]; and (ii) number of procambium cells in stems increases following treatment with TDIF [10]. However, proliferation of cambium is not abrogated in *pxy* suggesting existence of functionally redundant signaling mechanisms. Recently, other receptor kinases were implicated in the regulation of cambium proliferation, e.g. PXY correlated PXC [78] and REDUCED IN LATERAL GROWTH1 [79]. It is also plausible that cambium is regulated by as yet uncharacterized signaling modules. The limited experimental data on these signaling processes precludes adding them to CARENET at present. It would be desirable to incorporate these nodes as more information becomes available.

2. Many of the nodes in CARENET represent not a single gene, but a gene family with overlapping expression pattern, e.g. *ARF, RRA, WRKY, ERF*. Some members of these families may even have antagonistic functions. For example whilst AHPs are generally positive regulators of CK response, AHP6 inhibits CK signaling [39]. Functional redundancy could also confound determining the function and downstream targets of some nodes. The CARENET could be further refined once functions of the members of gene families are determined experimentally.

3. Our current model takes into account only external GA; however intracellular homeostasis of GA could also be important for cambium activity. The importance of the internally produced GA on secondary growth remains unknown. Filling this knowledge gap would establish the feedback loop for GA and introduce additional edges connecting GA loop to other parts of the network.

Conclusions

This work aims at understanding regulation of cambium proliferation by hormonal signals. Addressing this problem experimentally is challenging because of pleiotropic effect of hormones on gene transcription. Appropriately selected mathematical modeling tools can facilitate both experimental design and interpretation of the experimental data. While analytical solutions can be effective for dealing with simple processes, complex multi-parametric phenomena are more efficiently addressed using simulations. We have constructed and computationally verified a Boolean deterministic network model for the regulation of cambium activity. Behavior of the CARENET corroborates published experimental data.

To quantify behavior of CARENET under different combinations of hormones, we have introduced and compared the average activity coefficients of genetic markers *WOX4* and *ATHB8* whose levels of expression are known to correlate strongly with proliferation. The average activity coefficients were computed using a method inspired

by classical statistical mechanics. The central idea of the method is to use ensemble averaging over an ensemble consisting of all final states attainable with a particular control state. In statistical mechanics, every initial condition is assigned a weight (the probability of occurrence of that condition), and then quantities of interest are averaged over the ensemble of all relevant initial conditions using the above probabilities as weights. In the present case, we propose to assign weights to each *final* state based on the number of different initial conditions leading to that state. Then, given a specific control state, the average activity of the markers is computed by (i) calculating their activity for each final state, and (ii) averaging these activities over the ensemble of the final states using the above assigned weights. The proposed ensemble averaging procedure is applicable to generic Boolean networks, and thus it may be of broad interest in computational biology.

Overall, our network accurately represents mutually inhibitory relationships between auxin and cytokinin as well as cooperation between gibberellic acid and brassinosteroids during cambium proliferation. CARENET can be used for predicting: (i) cambial activity in response to developmental cues; (ii) effect of mutations on gene transcription and cambium proliferation; (iii) co-expression of genes and genetic markers. In addition to resembling available experimental data, CARENET demonstrates that similar cambium proliferation activity can be achieved under multiple final states. Hence, individual cells in cambium and potentially other stem cell niches can have distinct molecular identities. Another important feature of CARENET is that it can be expanded to include components of other signaling pathways and ultimately be integrated with existing models of xylem and phloem differentiation to compose a comprehensive model of secondary growth. Such a model would enable predicting the key nodes that can be targeted in plant breeding programs for optimized yield and biomass quality. In particular, breeding trees with higher wood yield and more efficient sequestration of CO_2 from the atmosphere would both alleviate the greenhouse effect and augment wood production.

Acknowledgments

The authors are grateful to Deirdre Fahy for thoughtful notes and for proofreading the text. This project was supported by NIFA hatch project WNP00826 (to AS).

References

1. Sanio K. Uber die Grosse der Holzzellen bei der gemeinen Kiefer (Pinus silvestris). Jb. wiss. Bot.(8). 1872:401-20.

2. Agusti J, Greb T. Going with the wind–adaptive dynamics of plant secondary meristems. Mechanisms of development. 2013 Jan 31;130(1):34-44.

3. Milhinhos A, Miguel CM. Hormone interactions in xylem development: a matter of signals. Plant cell reports. 2013 Jun 1;32(6):867-83.

4. Bhalerao RP, Fischer U. Auxin gradients across wood–instructive or incidental?. Physiologia plantarum. 2014 May 1;151(1):43-51.

5. Mähönen AP, Bonke M, Kauppinen L, Riikonen M, Benfey PN, Helariutta Y. A novel two-component hybrid molecule regulates vascular morphogenesis of the Arabidopsis root. Genes & development. 2000 Dec 1;14(23):2938-43.

6. Love J, Björklund S, Vahala J, Hertzberg M, Kangasjärvi J, Sundberg B. Ethylene is an endogenous stimulator of cell division in the cambial meristem of Populus. Proceedings of the National Academy of Sciences. 2009 Apr 7;106(14):5984-9.

7. Eriksson ME, Israelsson M, Olsson O, Moritz T. Increased gibberellin biosynthesis in transgenic trees promotes growth, biomass production and xylem fiber length. Nature biotechnology. 2000 Jul 1;18(7):784-8.

8. Oh MH, Sun J, Oh DH, Zielinski RE, Clouse SD, Huber SC. Enhancing Arabidopsis leaf growth by engineering the BRASSINOSTEROID INSENSITIVE1 receptor kinase. Plant physiology. 2011 Sep 1;157(1):120-31.

9. Agusti J, Herold S, Schwarz M, Sanchez P, Ljung K, Dun EA, et al. Strigolactone signaling is required for auxin-dependent stimulation of secondary growth in plants. Proceedings of the National Academy of Sciences. 2011 Dec 13;108(50):20242-7.

10. Hirakawa Y, Shinohara H, Kondo Y, Inoue A, Nakanomyo I, Ogawa M, et al. Non-cell-autonomous control of vascular stem cell fate by a CLE peptide/receptor system. Proceedings of the National Academy of Sciences. 2008 Sep 30;105(39):15208-13.

11. Whitford R, Fernandez A, De Groodt R, Ortega E, Hilson P. Plant CLE peptides from two distinct functional classes synergistically induce division of vascular cells. Proceedings of the National Academy of Sciences. 2008 Nov 25;105(47):18625-30.

12. Fisher K, Turner S. PXY, a receptor-like kinase essential for maintaining polarity during plant vascular-tissue development. Current Biology. 2007 Jun 19;17(12):1061-6.

13. Etchells JP, Provost CM, Mishra L, Turner SR. WOX4 and WOX14 act downstream of the PXY receptor kinase to regulate plant vascular proliferation independently of any role in vascular organisation. Development. 2013 May 15;140(10):2224-34.

14. Hirakawa Y, Kondo Y, Fukuda H. TDIF peptide signaling regulates vascular stem cell proliferation via the WOX4 homeobox gene in Arabidopsis. The Plant Cell. 2010 Aug 1;22(8):2618-29.

15. Suer S, Agusti J, Sanchez P, Schwarz M, Greb T. WOX4 imparts auxin responsiveness to cambium cells in Arabidopsis. The Plant Cell. 2011 Sep 1;23(9):3247-59.

16. Baima S, Nobili F, Sessa G, Lucchetti S, Ruberti I, Morelli G. The expression of the Athb-8 homeobox gene is restricted to provascular cells in Arabidopsis thaliana. Development. 1995 Dec 1;121(12):4171-82.

17. Baima S, Possenti M, Matteucci A, Wisman E, Altamura MM, Ruberti I, et al. The Arabidopsis ATHB-8 HD-zip protein acts as a differentiation-promoting transcription factor of the vascular meristems. Plant Physiology. 2001 Jun 1;126(2):643-55.

18. Ohashi-Ito K, Fukuda H. HD-Zip III homeobox genes that include a novel member, ZeHB-13 (Zinnia)/ATHB-15 (Arabidopsis), are involved in procambium and xylem cell differentiation. Plant and Cell Physiology. 2003 Dec 15;44(12):1350-8.

19. Etchells JP, Turner SR. The PXY-CLE41 receptor ligand pair defines a multifunctional pathway that controls the rate and orientation of vascular cell division. Development. 2010 Mar 1;137(5):767-74.

20. Benítez M, Hejátko J. Dynamics of cell-fate determination and patterning in the vascular bundles of Arabidopsis thaliana. PloS one. 2013 May 27;8(5):e63108.

21. Kondo Y, Ito T, Nakagami H, Hirakawa Y, Saito M, Tamaki T, et al. Plant GSK3 proteins regulate xylem cell differentiation downstream of TDIF–TDR signalling. Nature communications. 2014 Mar 24;5.

22. Ilegems M, Douet V, Meylan-Bettex M, Uyttewaal M, Brand L, Bowman JL, et al. Interplay of auxin, KANADI and Class III HD-ZIP transcription factors in vascular tissue formation. Development. 2010 Mar 15;137(6):975-84.

23. Ragni L, Hardtke CS. Small but thick enough–the Arabidopsis hypocotyl as a model to study secondary growth. Physiologia plantarum. 2014 Jun 1;151(2):164-71.

24. Etchells JP, Provost CM, Turner SR. Plant vascular cell division is maintained by an interaction between PXY and ethylene signalling. PLoS Genet. 2012 Nov 15;8(11):e1002997.

25. Gerttula S, Zinkgraf M, Muday GK, Lewis DR, Ibatullin FM, Brumer H, et al. Transcriptional and hormonal regulation of gravitropism of woody stems in Populus. The Plant Cell. 2015 Oct 1;27(10):2800-13.

26. Taylor-Teeples M, Lin L, de Lucas M, Turco G, Toal TW, Gaudinier A, et al. An Arabidopsis gene regulatory network for secondary cell wall synthesis. Nature. 2015 Jan 29;517(7536):571-5.

27. Kauffman SA. Metabolic stability and epigenesis in randomly constructed genetic nets. Journal of theoretical biology. 1969 Mar 31;22(3):437-67.

28. Kauffman S. Homeostasis and differentiation in random genetic control networks. Nature. 1969 Oct;224:177-8.

29. Kauffman S. The large scale structure and dynamics of gene control circuits: an ensemble approach. Journal of Theoretical Biology. 1974 Mar 1;44(1):167-90.

30. Kauffman SA. The origins of order: Self organization and selection in evolution. Oxford University Press, USA; 1993.

31. Shmulevich I, Dougherty ER. Genomic signal processing. Princeton University Press; 2014 Sep 8.

32. Shmulevich I, Dougherty ER. Probabilistic Boolean networks: the modeling and control of gene regulatory networks. siam; 2010.

33. Veliz-Cuba A, Aguilar B, Laubenbacher R. Dimension reduction of large sparse AND-NOT network models. Electronic Notes in Theoretical Computer Science. 2015 Sep 16;316:83-95.

34. Wittmann DM, Krumsiek J, Saez-Rodriguez J, Lauffenburger DA, Klamt S, Theis FJ. Transforming Boolean models to continuous models: methodology and application to T-cell receptor signaling. BMC systems biology. 2009 Sep 28;3(1):1.

35. Sankar M, Osmont KS, Rolcik J, Gujas B, Tarkowska D, Strnad M, et al. A qualitative continuous model of cellular auxin and brassinosteroid signaling and their crosstalk. Bioinformatics. 2011 May 15;27(10):1404-12.

36. Voß U, Bishopp A, Farcot E, Bennett MJ. Modelling hormonal response and development. Trends in plant science. 2014 May 31;19(5):311-9.

37. Etchells JP, Mishra LS, Kumar M, Campbell L, Turner SR. Wood formation in trees is increased by manipulating PXY-regulated cell division. Current Biology. 2015 Apr 20;25(8):1050-5.

38. Hejátko J, Ryu H, Kim GT, Dobešová R, Choi S, Choi SM, et al. The histidine kinases CYTOKININ-INDEPENDENT1 and ARABIDOPSIS HISTIDINE KINASE2 and 3 regulate vascular tissue development in Arabidopsis shoots. The Plant Cell. 2009 Jul 1;21(7):2008-21.

39. Mähönen AP, Bishopp A, Higuchi M, Nieminen KM, Kinoshita K, Törmäkangas K, et al. Cytokinin signaling and its inhibitor AHP6 regulate cell fate during vascular development. Science. 2006 Jan 6;311(5757):94-8.

40. Matsumoto-Kitano M, Kusumoto T, Tarkowski P, Kinoshita-Tsujimura K, Václavíková K, Miyawaki K, et al. Cytokinins are central regulators of cambial activity. Proceedings of the National Academy of Sciences. 2008 Dec 16;105(50):20027-31.

41. Hirose N, Takei K, Kuroha T, Kamada-Nobusada T, Hayashi H, Sakakibara H. Regulation of cytokinin biosynthesis, compartmentalization and translocation. Journal of Experimental Botany. 2008;59(1):75-83.

42. Bishopp A, Lehesranta S, Vatén A, Help H, El-Showk S, Scheres B, et al. Phloem-transported cytokinin regulates polar auxin transport and maintains vascular pattern in the root meristem. Current Biology. 2011 Jun 7;21(11):927-32.

43. Hass C, Lohrmann J, Albrecht V, Sweere U, Hummel F, Yoo SD, et al. The response regulator 2 mediates ethylene signalling and hormone signal integration in Arabidopsis. The EMBO journal. 2004 Aug 18;23(16):3290-302.

44. De Rybel B, Möller B, Yoshida S, Grabowicz I, de Reuille PB, Boeren S, et al. A bHLH complex controls embryonic vascular tissue establishment and indeterminate growth in Arabidopsis. Developmental Cell. 2013 Feb 25;24(4):426-37.

45. Little CA, MacDonald JE, Olsson O. Involvement of Indole-3-Acetic Acid in Fascicular and Interfascicular Cambial Growth and Interfascicular Extraxylary Fiber Differentiation in Arabidopsis thaliana Inflorescence Stems. International Journal of Plant Sciences. 2002 Jul;163(4):519-29.

46. Peer WA. From perception to attenuation: auxin signalling and responses. Current opinion in plant biology. 2013 Oct 31;16(5):561-8.

47. Zažímalová E, Murphy AS, Yang H, Hoyerová K, Hošek P. Auxin transporters–why so many?. Cold Spring Harbor perspectives in biology. 2010 Mar 1;2(3):a001552.

48. Ding Z, Wang B, Moreno I, Dupláková N, Simon S, Carraro N, et al. ER-localized auxin transporter PIN8 regulates auxin homeostasis and male gametophyte development in Arabidopsis. Nature communications. 2012 Jul 3;3:941.

49. Sawchuk MG, Edgar A, Scarpella E. Patterning of leaf vein networks by convergent auxin transport pathways. PLoS Genet. 2013 Feb 21;9(2):e1003294.

50. Bishopp A, Help H, El-Showk S, Weijers D, Scheres B, Friml J, et al. A mutually inhibitory interaction between auxin and cytokinin specifies vascular pattern in roots. Current Biology. 2011 Jun 7;21(11):917-26.

51. De Rybel B, Adibi M, Breda AS, Wendrich JR, Smit ME, Novák O, et al. Integration of growth and patterning during vascular tissue formation in Arabidopsis. Science. 2014 Aug 8;345(6197):1255215.

52. Werner T, Köllmer I, Bartrina I, Holst K, Schmülling T. New insights into the biology of cytokinin degradation. Plant Biology. 2006 May;8(03):371-81.

53. Nordström A, Tarkowski P, Tarkowska D, Norbaek R, Åstot C, Dolezal K, et al. Auxin regulation of cytokinin biosynthesis in Arabidopsis thaliana: a factor of potential importance for auxin–cytokinin-regulated development. Proceedings of the National Academy of Sciences of the United States of America. 2004 May 25;101(21):8039-44.

54. Tanaka M, Takei K, Kojima M, Sakakibara H, Mori H. Auxin controls local cytokinin biosynthesis in the nodal stem in apical dominance. The Plant Journal. 2006 Mar 1;45(6):1028-36.

55. Schlereth A, Möller B, Liu W, Kientz M, Flipse J, Rademacher EH, et al. MONOPTEROS controls embryonic root initiation by regulating a mobile transcription factor. Nature. 2010 Apr 8;464(7290):913-6.

56. Ioio RD, Nakamura K, Moubayidin L, Perilli S, Taniguchi M, Morita MT, et al. A genetic framework for the control of cell division and differentiation in the root meristem. Science. 2008 Nov 28;322(5906):1380-4.

57. Pernisová M, Klíma P, Horák J, Válková M, Malbeck J, Souček P, et al. Cytokinins modulate auxin-induced organogenesis in plants via regulation of the auxin efflux. Proceedings of the National Academy of Sciences. 2009 Mar 3;106(9):3609-14.

58. Růžička K, Šimášková M, Duclercq J, Petrášek J, Zažímalová E, Simon S, et al. Cytokinin regulates root meristem activity via modulation of the polar auxin transport. Proceedings of the National Academy of Sciences. 2009 Mar 17;106(11):4284-9.

59. Šimášková M, O'Brien JA, Khan M, Van Noorden G, Ötvös K, Vieten A, et al. Cytokinin response factors regulate PIN-FORMED auxin transporters. Nature communications. 2015 Nov 6;6.

60. Ckurshumova W, Smirnova T, Marcos D, Zayed Y, Berleth T. Irrepressible MONOPTEROS/ARF5 promotes de novo shoot formation. New Phytologist. 2014 Nov 1;204(3):556-66.

61. Liu L, Zinkgraf M, Petzold HE, Beers EP, Filkov V, Groover A. The Populus ARBORKNOX1 homeodomain transcription factor regulates woody growth through binding to evolutionarily conserved target genes of diverse function. New Phytologist. 2015 Jan 1;205(2):682-94.

62. Liebsch D, Sunaryo W, Holmlund M, Norberg M, Zhang J, Hall HC, et al. Class I KNOX transcription factors promote differentiation of cambial derivatives into xylem fibers in the Arabidopsis hypocotyl. Development. 2014 Nov 15;141(22):4311-9.

63. Caño-Delgado A, Yin Y, Yu C, Vafeados D, Mora-García S, Cheng JC, et al. BRL1 and BRL3 are novel brassinosteroid receptors that function in vascular differentiation in Arabidopsis. Development. 2004 Nov 1;131(21):5341-51.

64. Oh MH, Wang X, Kota U, Goshe MB, Clouse SD, Huber SC. Tyrosine phosphorylation of the BRI1 receptor kinase emerges as a component of brassinosteroid signaling in Arabidopsis. Proceedings of the National Academy of Sciences. 2009 Jan 13;106(2):658-63.

65. Wang, Z.Y., T. Nakano, J. Gendron, J.X. He, M. Chen, D. Vafeados, Y.L. Yang, S. Fujioka, S. Yoshida, T. Asami, and J. Chory. 2002. Nuclear-localized BZR1 mediates brassinosteroid-induced growth and feedback suppression of brassinosteroid biosynthesis. Developmental cell. 2:505-513.

66. Wang ZY, Nakano T, Gendron J, He J, Chen M, Vafeados D, et al. Nuclear-localized BZR1 mediates brassinosteroid-induced growth and feedback suppression of brassinosteroid biosynthesis. Developmental cell. 2002 Apr 30;2(4):505-13.

67. Wang H, Avci U, Nakashima J, Hahn MG, Chen F, Dixon RA. Mutation of WRKY transcription factors initiates pith secondary wall formation and increases stem biomass in dicotyledonous plants. Proceedings of the National Academy of Sciences. 2010 Dec 21;107(51):22338-43.

68. Björklund S, Antti H, Uddestrand I, Moritz T, Sundberg B. Cross-talk between gibberellin and auxin in development of Populus wood: gibberellin stimulates polar auxin transport and has a common transcriptome with auxin. The Plant Journal. 2007 Nov 1;52(3):499-511.

69. Ragni L, Nieminen K, Pacheco-Villalobos D, Sibout R, Schwechheimer C, Hardtke CS. Mobile gibberellin directly stimulates Arabidopsis hypocotyl xylem expansion. The Plant Cell. 2011 Apr 1;23(4):1322-36.

70. Bornholdt S. Boolean network models of cellular regulation: prospects and limitations. Journal of the Royal Society Interface. 2008 Aug 6;5(Suppl 1):S85-94.

71. Krawitz P, Shmulevich I. Basin entropy in Boolean network ensembles. Physical review letters. 2007 Apr 9;98(15):158701.

72. Ji J, Strable J, Shimizu R, Koenig D, Sinha N, Scanlon MJ. WOX4 promotes procambial development. Plant physiology. 2010 Mar 1;152(3):1346-56.

73. Donner TJ, Sherr I, Scarpella E. Regulation of preprocambial cell state acquisition by auxin signaling in Arabidopsis leaves. Development. 2009 Oct 1;136(19):3235-46.

74. Furuta KM, Hellmann E, Helariutta Y. Molecular control of cell specification and cell differentiation during procambial development. Annual review of plant biology. 2014 Apr 29;65:607-38.

75. Lucas WJ, Groover A, Lichtenberger R, Furuta K, Yadav SR, Helariutta Y, et al. The plant vascular system: evolution, development and functions. Journal of Integrative Plant Biology. 2013 Apr 1;55(4):294-388.

76. Jouannet V, Brackmann K, Greb T. (Pro)cambium formation and proliferation: two sides of the same coin?. Current opinion in plant biology. 2015 Feb 28;23:54-60.

77. Lavenus J, Goh T, Guyomarc'h S, Hill K, Lucas M, Voß U, et al. Inference of the Arabidopsis lateral root gene regulatory network suggests a bifurcation mechanism that defines primordia flanking and central zones. The Plant Cell. 2015 May 1;27(5):1368-88.

78. Wang J, Kucukoglu M, Zhang L, Chen P, Decker D, Nilsson O, et al. The Arabidopsis LRR-RLK, PXC1, is a regulator of secondary wall formation correlated with the TDIF-PXY/TDR-WOX4 signaling pathway. BMC plant biology. 2013 Jul 1;13(1):1.

79. Agusti J, Lichtenberger R, Schwarz M, Nehlin L, Greb T. Characterization of transcriptome remodeling during cambium formation identifies MOL1 and RUL1 as opposing regulators of secondary growth. PLoS Genet. 2011 Feb 17;7(2):e1001312.

Supporting Information

S1 Fig. Simulation of the CARENET which results in a stable state at step 26 shown in Figure 3A. Control nodes CK0, IAA0, EHTL and TDIF are on.

S2 Fig. An example of limit cycle where cytokinin (CK0), auxin (IAA0), and brassinosteroids are on. The cycle of 6 steps long establishes at step 9. Brackets indicate single cycles.

S3 Fig. An example of limit cycle where cytokinin (CK0), auxin (IAA0), and brassinosteroids are on. The cycle of 6 steps long establishes at step 9. Brackets indicate single cycles.

S4 Fig. Two structurally distinct limit cycles with high proliferation activity ($\overline{\alpha}_{\mathbf{c}}(C) > 0.75$) generated by identical set of controls.

S1 Table. Rules for calculating the status of each node in the CARENET. The rules are inferred form the experimental evidence shown in S2 Table.

S2 Table. Experimental evidence supporting interactions between nodes of CARENET.

S3 Table. Statistical analysis of all stable states generated by the CARENET.